ANDRZEJ KOZŁOWSKI, ŁUKASZ KARWOWSKI & WIESŁAW OLSZYŃSKI

Tungsten-tin-molybdenum mineralization in the Karkonosze massif

ABSTRACT: Ore mineralization in the zone of aplogranites in the NW part of the Karkonosze massif (Sudetes Mts), partly metasomatized by Na-bearing solutions, and in quartz veins, reveal a lengthly list of minerals, such as wolframite, cassiterite, molybdenite, scheelite, native bismuth, bismuthite and bismuth sulfosalts. Studies of fluid inclusions reveal the crystallization conditions as: pressure about 700 atm, temperatures 405—375°C in the pneumatolytic stage and, after condensation, from 375°C down to about 100°C (hydrothermal stage). The mineral assemblage, as well as the sequence and conditions of crystallization are typical of the majority of W-Sn-Mo deposits.

INTRODUCTION

In marginal zones of the Karkonosze granitoid massif (Sudetes), the W-Sn-Mo mineralization has been found in aplogranite and associated quartz veins. The mineralized aplogranite is exposed at a granite quarry, about 4 km west of Szklarska Poręba (cf. Fig. 1 and Karwowski, Olszyński & Kozłowski 1973). The aplogranite/monzonitic granite contact is clearly intrusive. Ore minerals appear mainly in quartz veins occurring in deeper parts of aplogranite and they are disseminated in aplogranite especially inside numerous small voids. Mineralized veins are 0.5 to 2.5 cm thick (Fig. 2) and dipping declivitously at a strike of about 40°.

Fig. 1. Sketch-map of the Karkonosze massif

1 — aplogranite, 2 — granite, 3 — rock series of the Kaczawa Mts, 4 — metamorphic series of eastern crust of the massif, 5 — Izera gneiss, 6 — mica schist and hornfels, 7 — granite quarry with ore-bearing aplogranites at Szklarska Poręba Huta

INVESTIGATING METHODS

The ore parageneses were studied by the methods of a transmitted and reflected light microscopy. Temperatures were measured by the homogenization and decrepitation of fluid inclusions. Decomposition temperatures were taken from Naumov (1968) or determined by the DTA method using the MOM derivatograph. Pressures were found from the homogenization and decrepitation data by the Naumov & Malinin (1968) method. The X-ray analysis was made on the DRON diffractometer using CuKα radiation, and IR absorption spectra were taken on the UR — 20 spectrophotometer. The wolframite density was determined, by the picnometer method, at 23°C. The composition was analyzed by the chemical and spectral emission methods. The chemical composition of inclusions was determined after Kalyuzhnyi (1960) by the method of water leachates.

PETROGRAPHY

Aplogranites differ macro- and microscopically from the surrounding monzonitic granite. They are enriched in quartz, slightly also in plagioclase, but are poorer in biotite and partly in potassium feldspar. The last--named is often twinned and perthitized, and sometimes larger albite patches become chessboarded (Pl. 1, Fig. 1). Plagioclases (oligoclase to andesine) have outer rims consisting of albite (Pl. 1, Fig. 2). In addition, the metasomatic albite (Pl. 1, Fig. 3) occurs together with a strongly

chloritized biotite. There also occurs primary chlorite of the hydrothermal origin (Pl. 4, Fig. 3). Quartz is partly similar to that from granite and partly forms granophyric intergrowths (Pl. 4, Fig. 1). The rock is cut by quartz veins that bear ore minerals (Pl. 4, Fig. 2) and relics of feldspars. Accessory minerals as epidote, sphene, apatite and zircon, are subordinate.

FLUID INCLUSIONS

Some generations of fluid inclusions were found in quartz and cleavelandite of pegmatites in granite and of veins and druses bearing ore minerals in aplogranite (Pls 2 and 3). Homogenization temperatures and inclusion generations are given in the explanations of Plates 2 and 3. The inclusion studies reveal in the early stage of mineralization the existence of pneumatolytic conditions with the resulting condensation at temperatures between 380 and 370°C. The well developed hydrothermal stage lasts down to temperatures lower than 110°C. At temperatures of about 0°C neither CO_2 nor salts were found; the parageneses crystallized from relatively strongly diluted solutions bearing Na, Ca, K, Al, Cl ($n \cdot 10^0$ %), Li, Fe, F ($n \cdot 10^{-1}$ %), Ba, Ga, Ti, Mn, W, Bi, BO_3^{3-} ($n \cdot 10^{-2}$ %), Mg, Sn, Be ($n \cdot 10^{-3}$ %). In quartz grains of aplogranite, the very small inclusions (tenths of micrometer in diameter) probably contain a silicate melt. In addition, all kinds of inclusions, occurring in ore parageneses, were ascertained in the same grains.
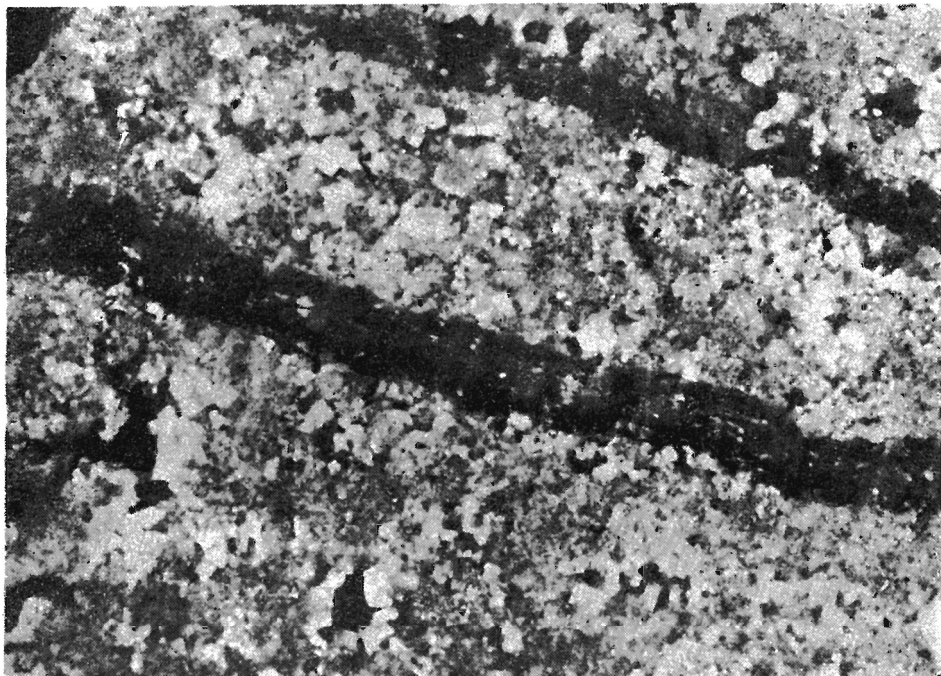

Fig. 2. Aplogranite with voids and quartz veins; in veins relics of feldspars (white) are visible; × 1.5

A decrepitation analysis was performed on wolframite, cassiterite, molybdenite, magnetite *II*, pyrrhotite, chalcopyrite *I*, bismuthite, pyrite, feldspar from vugs and quartz (Fig. 3).
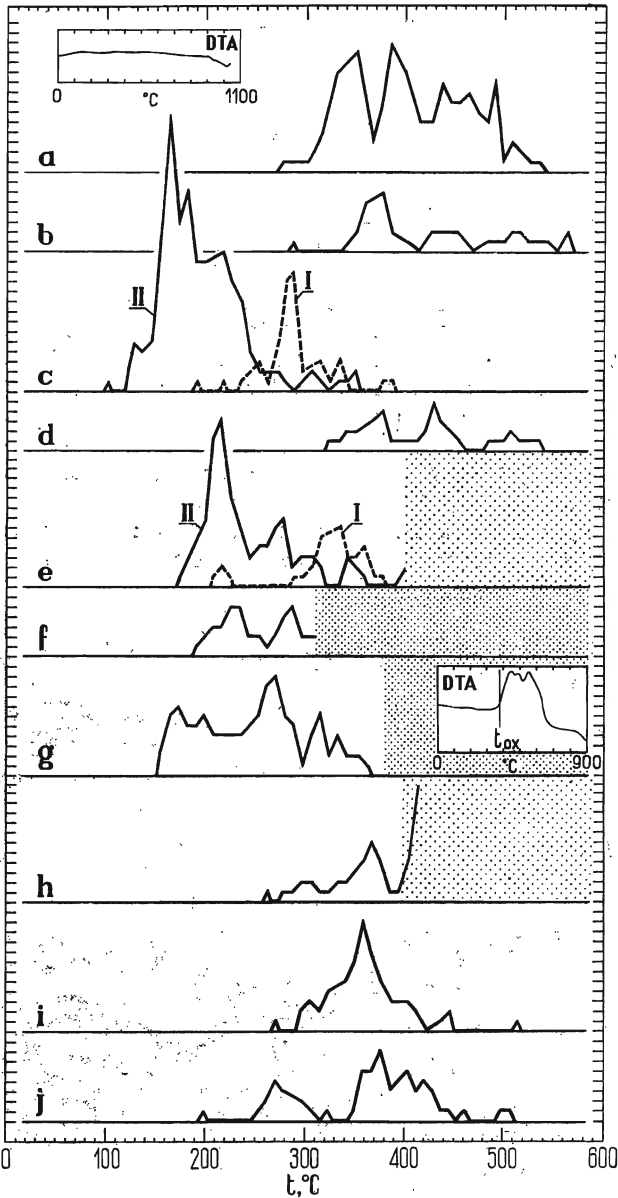

Fig. 3. Decrepigraphs of minerals from Szklarska Poręba Huta
a — wolframite (DTA curve enclosed), b — cassiterite, c — molybdenite (generation *I* and *II*) from veins, d — magnetite *II*, e — pyrrhotite from voids (*I*) and from veins (*II*), f — chalcopyrite, g — bismuthite (DTA curve enclosed), h — pyrite, i — feldspar from void, j — quartz from void; temperature range above mineral oxidation is dotted; on the intensity scale, one section equals one impulse
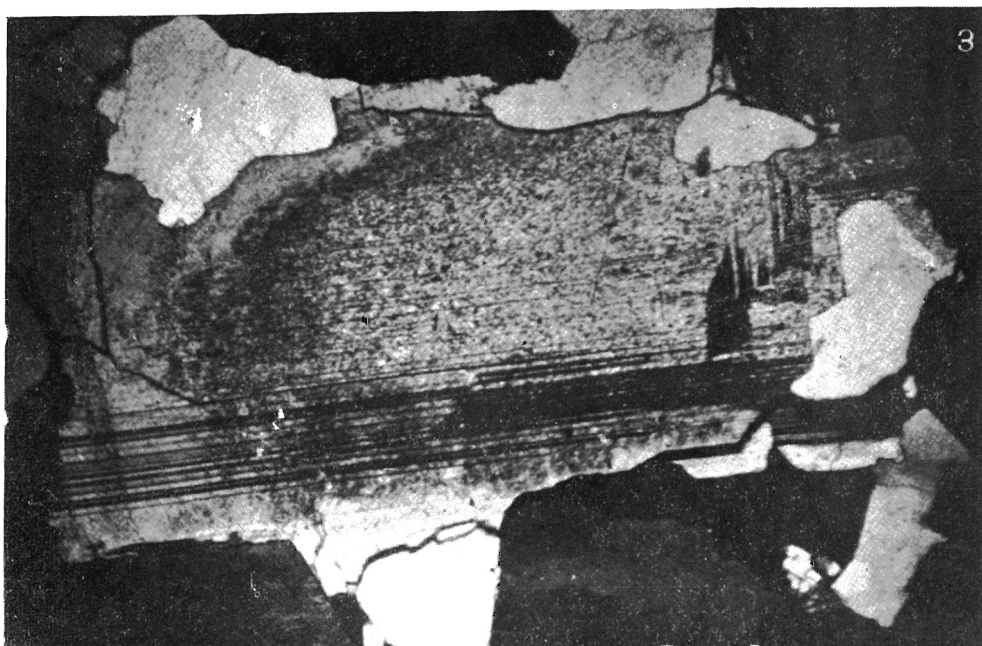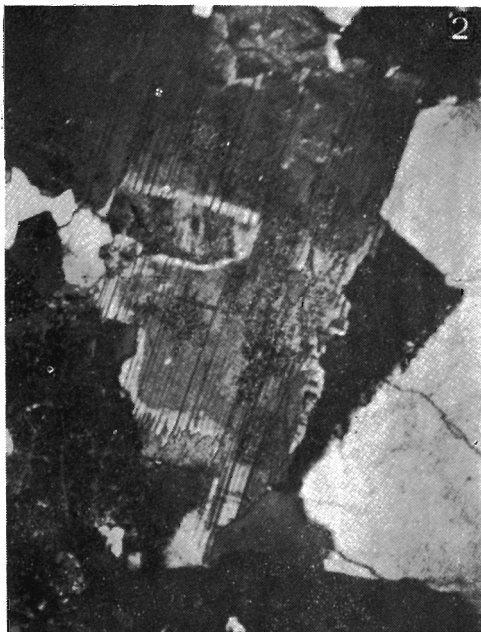
1 — Perthite partly altered into chessboard albite; nicols oblique, $\times$ 120.
2 — Oligoclase An_{17} surrounded by thin rim of albite An_3; nicols crossed, $\times$ 70.
3 — Pseudomorph (inner part strongly sericitized) of albite An_0 after primarily zonated plagioclase; nicols crossed, $\times$ 110.
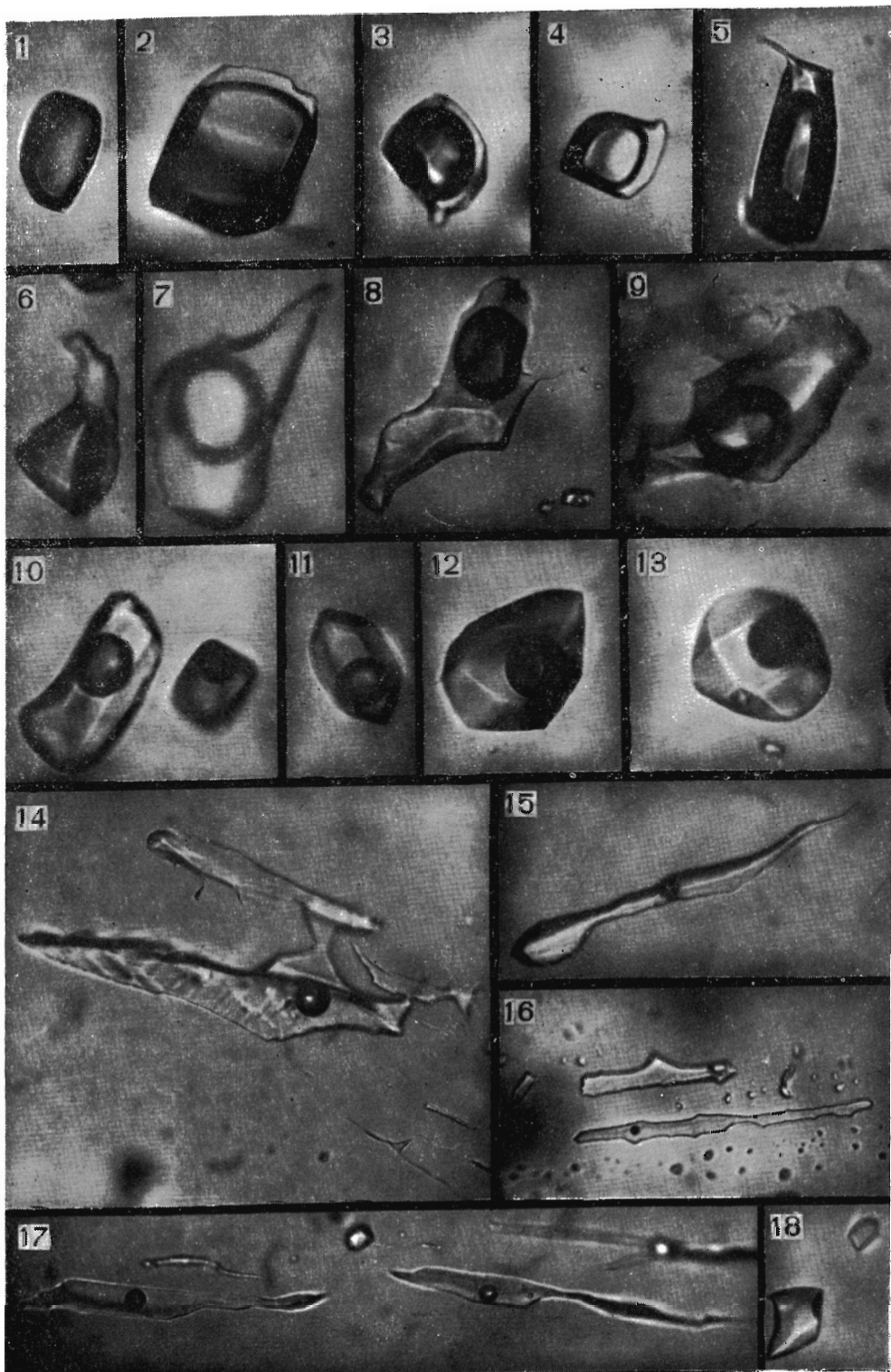
Fluid inclusions in quartz from pegmatitic druses, × 1000: **1-4** — liquid-gaseous, T_h 480—380°C, *I* generation; **5-7** — gaseous-liquid, T_h 360—300°C, *II* generation; **8-10** — gaseous-liquid, T_h 270—200°C, *III* generation; **11-13** — gaseous-liquid, T_h 160—110°C, *IV* generation

Inclusions in cleavelandite, × 2000; **14** — gaseous-liquid, T_h 290°C; **15-16** — gaseous--liquid, T_h 80°C
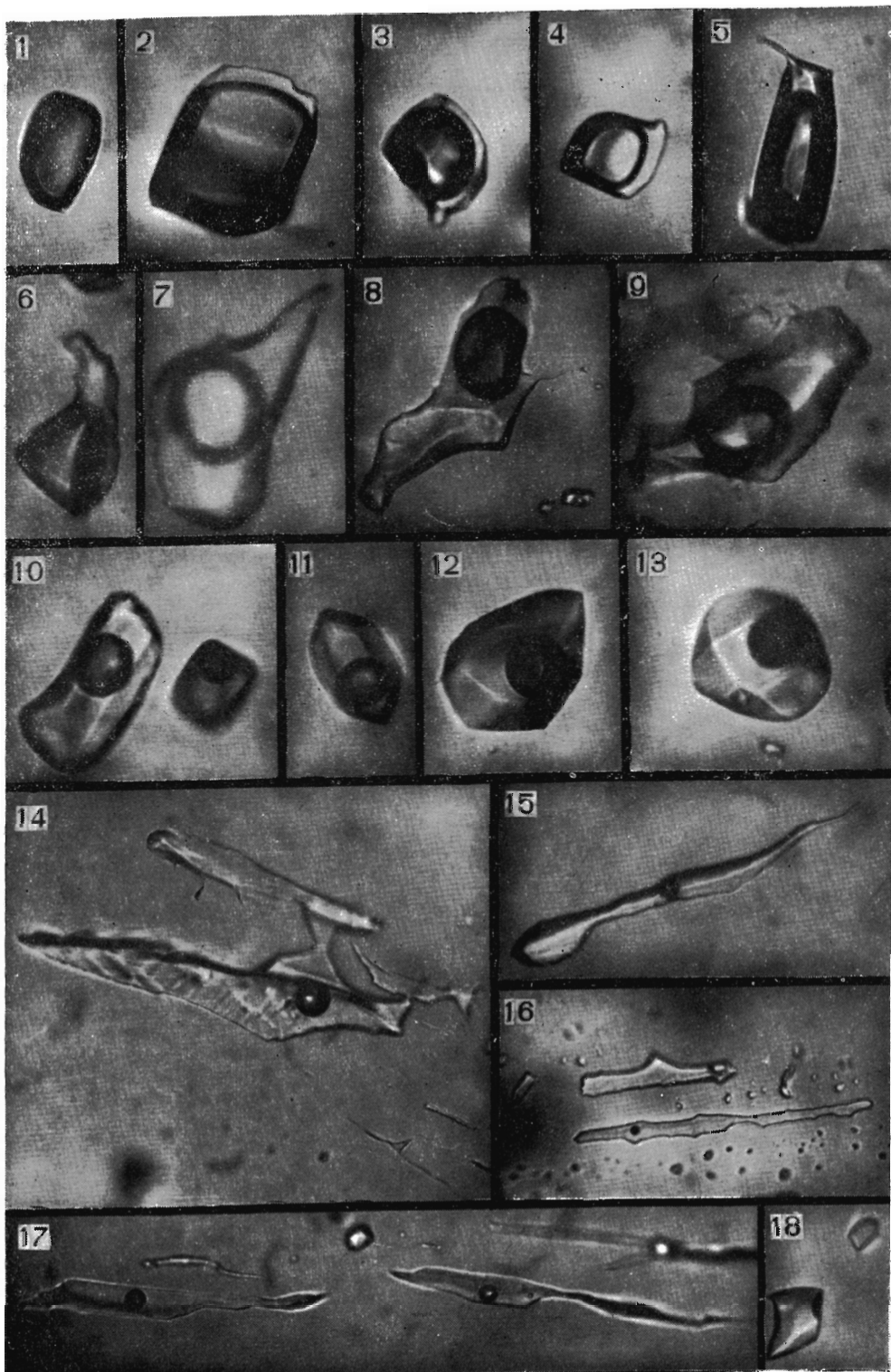
Fluid inclusions in quartz from pegmatitic druses, $\times$ 1000: **1-4** — liquid-gaseous, T_h 480—380°C, *I* generation; **5-7** — gaseous-liquid, T_h 360—300°C, *II* generation; **8-10** — gaseous-liquid, T_h 270—200°C, *III* generation; **11-13** — gaseous-liquid, T_h 160—110°C, *IV* generation

Inclusions in cleavelandite, $\times$ 2000; **14** — gaseous-liquid, T_h 290°C; **15-16** — gaseous-liquid, T_h 80°C
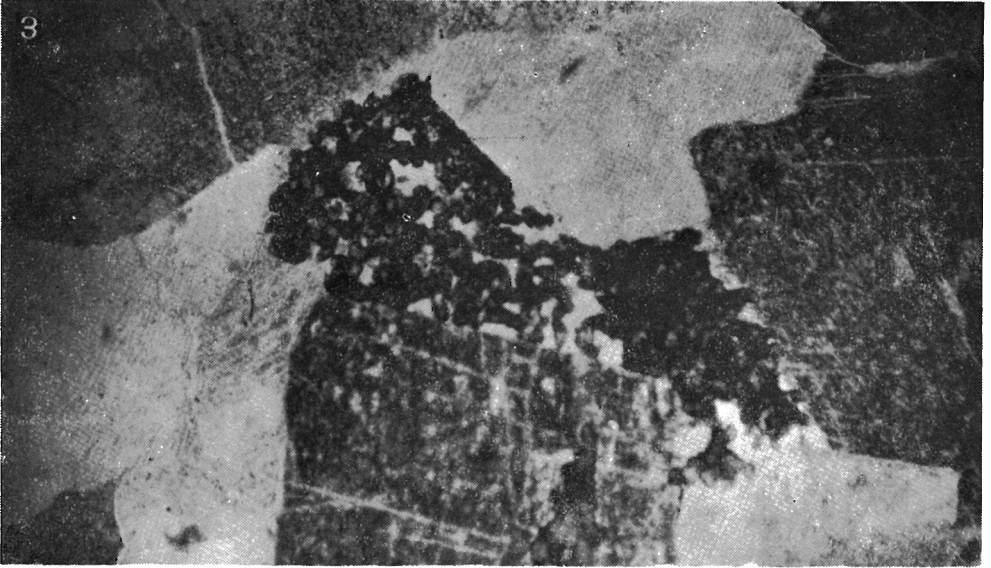
1 — Granophyric structure of aplogranite; nicols crossed, × 80.
2 — Grains of ore mineral (probably wolframite) in quartz veinlet cutting aplogranite; nicols oblique, × 120.
3 — Spherolitic aggregates of hydrothermal chlorite (in central part), surrounded by strongly sericitized perthites; nicols oblique, × 100.

Inclusions homogenizing at temperatures about 300°C yielded pressures of 725 atm (± 10%) and those homogenizing at about 200°C — 680 atm (± 10%).

MAIN MINERALOGICAL AND GEOCHEMICAL FEATURES

There occur some differences in chemical composition between the monzonitic granite and aplogranite (Table 1). The latter is enriched in SiO_2 and alkalies and bears lower amounts of TiO_2, FeO, Fe_2O_3, CaO and MgO, probably resulting from primary differences of parent melt and moderate sodium metasomatosis.

Table 1

Chemical composition of monzonitic granite and aplogranite (wt. %)

Component	Monzonitic granite	Aplo-granite
SiO_2	72.32	74.61
Al_2O_3	13.10	14.22
Fe_2O_3	1.91	0.59
FeO	1.86	0.53
MgO	0.58	0.38
CaO	1.48	1.00
Na_2O	3.00	3.50
K_2O	4.86	5.04
TiO_2	0.17	0.04
MnO	0.04	0.03
H_2O^+	0.46	0.35
H_2O^-	0.17	0.10
Total	99.95	100.39

Trace elements of biotites (Table 2) indicate, that the origin of aplogranite was similar to that of pegmatites rather than to the *sensu stricto* magmatic granite crystallization. The tin content of the biotites supports the supposition that parent rocks, in particular aplogranites, are tin-bearing.

Table 2

Trace elements in biotites (wt. %)
Analysed by Dr. P. Zawidzki

Element	Biotite from granite	Biotite from aplogranite	Biotites from pegmatite	
Ba	0.08	0.008	0.005	0.005
Sr	0.0035	0.0058	0.0033	0.002
Sc	0.013	0.012	0.014	0.028
Cr	0.012	0.001	0.001	0.001
Co	0.0015	0.0008	0.001	0.0008
Ni	0.0025	0.001	0.0012	0.0015
V	0.03	0.006	0.018	0.007
Sn	0.02	0.035	0.016	0.022
Pb	0.002	0.002	0.002	0.002

Among the trace elements of pyrite and chalcopyrite (Table 3), the distinct domination of Co over Ni seems to result from a relatively high temperature of the origin of these sulfides (cf. Polański & Smulikowski 1969). The relatively higher amount of gallium in sulfides, particularly in pyrrhotite, is apparent here. The presence of such elements as Ti, Zn, Ag, Cu, Mo, Mn, Sn, Pb, As and Sb may be caused by mineral inclusions or by structural admixtures.

Element	Pyrrhotite	Pyrite	Chalcopyrite
Co	0.0073	0.02	0.01
Ni	0.0046	0.0039	0.0043
Ti	0.0130	0.0096	0.0095
Zn	0.021	0.011	0.022
Ag	0.0028	0.0054	0.1
Cu	>1	>1	>10
V	0.0059	0.0012	0.0029
Mo	0.0015	0.0012	0.002
Mn	0.008	0.0042	0.021
Ga	0.011	0.0048	0.0054
Sn	0.0087	0.0022	0.014
Pb	0.017	0.05	0.046
As	0.00	0.02	0.02
In	~0.001	~0.001	~0.001
Sb	~0.001	~0.001	~0.001

Not detected: Ge, Tl, Cr, Au, W, Y, Cd

Table 3

Trace elements in sulfides (wt.%) Analysed by T. Wesołowska, M. Sc.

The analysis of wolframites (Table 4) reveals that they are true Fe-wolframites, poor in Nb, which, however, strongly prevails over Ta as a result of crystallization in rocks submitted to a sodium metasomatosis.

Table 4

Chemical composition (wt. %) and density of wolframites from Szklarska Poręba Huta

	Wolframite from void	Wolframite from vein	Wolframite intergrown with scheelite from vein
FeO	18.11	16.42	13.6
MnO	5.31	7.01	5.8
WO_3	76.49	76.48	73.8
CaO	traces	traces	2.7
insoluble in aqua regia	–	–	3.1
Nb	0.001–0.01	0.001–0.01	0.001–0.01
Ta	0.00	0.00	0.0001
Sc	0.003	0.003	0.003
$MnWO_4$	22.6	29.9	24.7
$CaWO_4$	–	–	13.9
Density g/cm³	7.26	7.14	6.85

During pneumatolytic-hydrothermal processes, Nb is usually accompanied by Sc, which also accumulates in wolframites. Determined amounts of Sc set in ranges of 0.001 to 0.01%, are most frequently reported in literature (Barabanov & Syritso 1966; Syritso 1967; Maksimiuk 1971; Sotnikov & Nikitina 1971). On the diagram: wolframite composition versus wolframite density (Fig. 4), the studied mineral falls in the area poor in Nb-Ta admixtures and with lowered density.
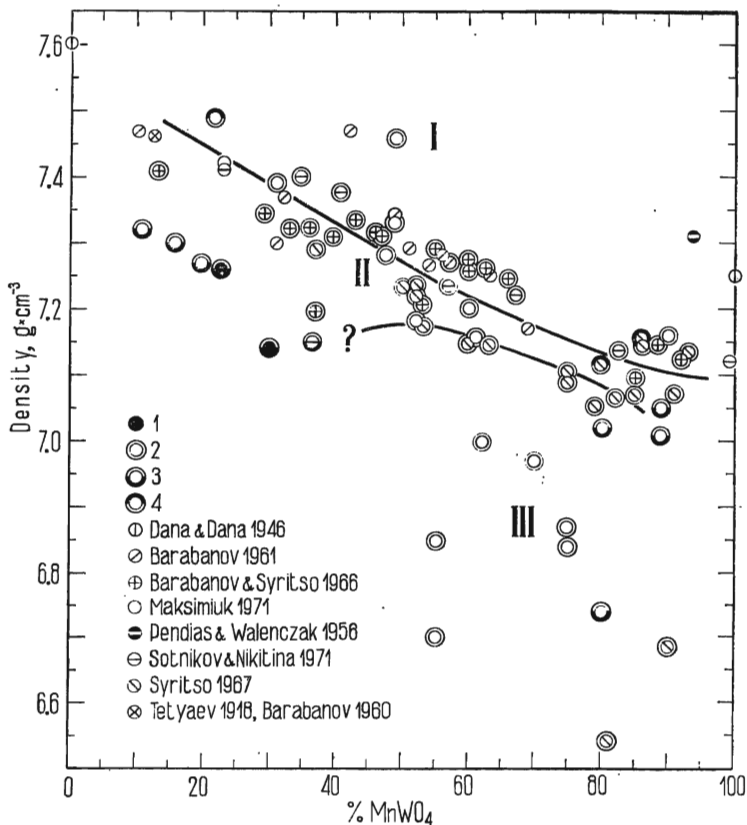

Fig. 4. Relationship between composition and density of wolframite (*after* Barabanov & Syritso 1966; Maksimiuk 1971; changed and completed)
I — Nb$_2$O$_5$ amount 0.0—0.3 wt%, *II* — Nb$_2$O$_5$ amount 0.31—0.7 wt%, *III* — Nb$_2$O$_5$ amount > 0.71 wt%
1 — wolframites from Szklarska Poręba Huta, 2 — Nb$_2$O$_5$ amount inside adequate ranges, 3 — Nb$_2$O$_5$ amount lowered, 4 — Nb$_2$O$_5$ amount highered

The IR-absorption analysis (Fig. 5) allows one to ascertain that the tungsten mineral is Fe-wolframite (low intensity of 425 and 460 cm^{-1} bands, cf. Moenke 1960) with varying admixture of scheelite, as indicated by the band 445 cm^{-1}.

The results of the above investigations were confirmed by X-ray powder patterns (Fig. 6a), due to which molybdenite and bismuthite were also identified (Fig. 6b and 6c).

MINERAL SUCCESSION

Wolframite and scheelite occur both in quartz veins (Fig. 7) and voids of aplogranite. The wolframite crystals in veins are zonated, up to 50 mm long (Pl. 5, Figs 1—3) and usually euhedral. In aplogranite, wolframite forms anhedral crystals without zonation (Pl. 5, Fig. 4) and it appears in aggregates reaching 3 cm in diameter. Wolframite is one of the earliest minerals in ore paragenesis and only in its later stage it crystallizes together with cassiterite, molybdenite, scheelite and pyrite. Scheelite was formed partly by the alteration of wolframite (Pl. 6, Figs 1, 3 and 4) and filled the interstices between wolframite grains (Pl. 7, Figs 1 and 2), being usually younger than wolframite and in part syngenetic with its last crystals.
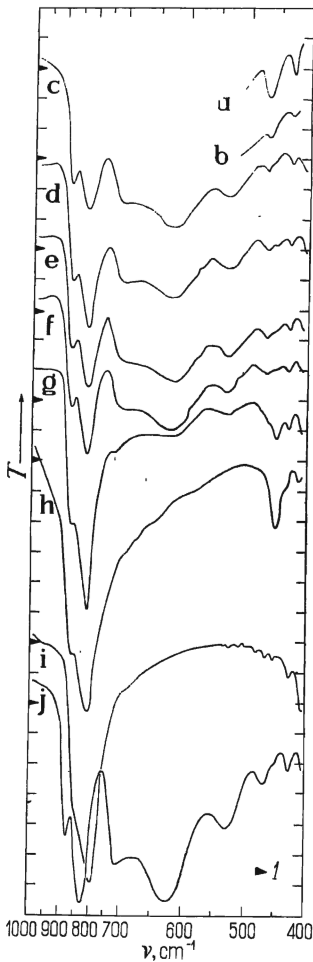
Fig. 5. The IR-absorption spectra of tungsten minerals

a — wolframite 82.24% $MnWO_4$, Kalgutinskoe, USSR (Sotnikov & Nikitina 1971, sample 123), b — wolframite 36.42% $MnWO_4$, Buguzunskoe, USSR (ibidem, sample 12), c — wolframite No. IGMiP 2057, Tinh Tuc, Vietnam, d — wolframite from vein, 29.9% $MnWO_4$, Szklarska Poręba, e—f other wolframites from veins, Szklarska Poręba, g — wolframite from void, Szklarska Poręba, h — scheelite No. IGMiP 3490, Cinovec, CSSR, i — scheelite No. IGMiP 3488, Atolia, California, j — huebnerite 93.7% $MnWO_4$, No. 157, Paszowice
KBr pellets, 0.66 mg of sample per 1 cm^2 of pellet

Cassiterite occurs together with wolframite in veins or in aplogranite, sometimes forming twinned crystals (Pl. 6, Figs 2—4).

Molybdenite in quartz veins crystallized after magnetite II, intergrowing with bismuthite and bismuth sulfosalts (Pl. 7, Fig. 3; Pl. 10, Fig. 4; Pl. 11, Fig. 1). It was

formed together with pyrrhotite (Pl. 7, Fig. 4), chalcopyrite *I*, native bismuth *I*, and, partly, with final wolframite crystals and scheelite.

Pyrite crystallized as euhedral or anhedral crystals (Pl. 7, Fig. 2) coeval with pyrrhotite and chalcopyrite *I* (Pl. 9, Fig. 4).

Magnetite forms two generations; the first occurs only in aplogranite as intergrowths with ilmenite lamellae (Pl. 8, Figs 1 and 3). Microscopic investigations reveal that these two minerals do not form exsolution structures, although magnetite *I* is a titaniferous variety, but that ilmenite lamellae crystallized primarily in biotite which afterwards turned into chlorite (Pl. 8, Figs 2 and 4). Post-biotitic chlorite was replaced by magnetite *I*, afterwards forming with ilmenite structures of pseudoexsolution. Similar ilmenite lamellae occur in pyrrhotite (Pl. 9, Fig. 1). In the neighborhood of pyrrhotite magnetite *I* probably passed into maghemite. Magnetite *II* frequently occurs in quartz veins with mushketovite (Pl. 10, Fig. 3; Pl. 11, Fig. 2) and bears a minor amount of Ti.

Pyrrhotite often occurs as lamellae of two varieties (monoclinic and hexagonal, *cf.* Arnold 1969) in one composite grain (Pl. 9, Fig. 3), neighboring with grains of simple, non-lamellar structure. This mineral was found together with chalcopyrite *I* (Pl. 9, Fig. 2), pyrite (Pl. 9, Fig. 4), native bismuth *I* and molybdenite (Pl. 7, Fig. 4), when the precipitation of wolframite was closed. Pyrrhotite is often replaced by melnikovite, then turned into pyrite (Pl. 8, Figs 3 and 4; Pl. 7, Fig. 4).
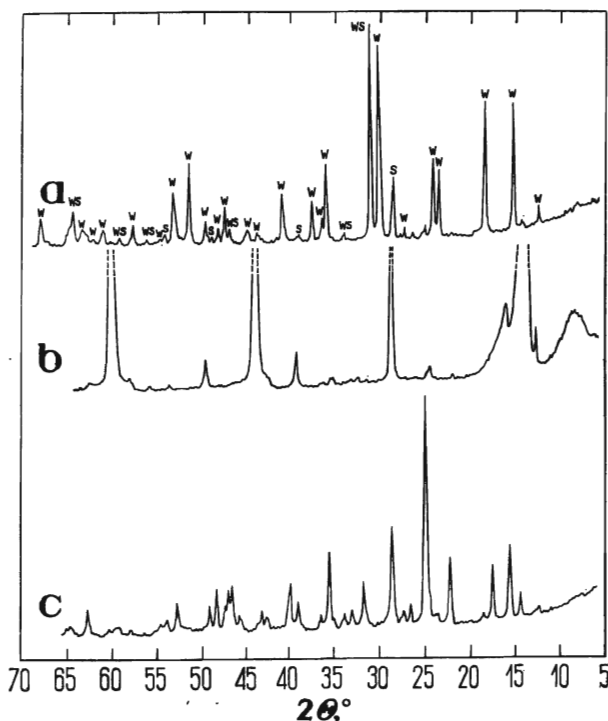
Fig. 6. The X-ray powder patterns of minerals from Szklarska Poręba Huta: **a** — wolframite (*w*) with scheelite (*s*), **b** — molybdenite, **c** — bismuthite

Chalcopyrite occurs as two generations. The first is anisotropic, twinned and bearing inclusions of sphalerite (Pl. 9, Fig. 2). It occurs in paragenesis with pyrite, bismuthite, bismuth sulfosalts and molybdenite; it is subsequent to magnetite II (Pl. 11, Fig. 2). The second, isotropic, occurs in altered parts of Bi-sulfosalts in paragenesis with native bismuth II.

Sphalerite is dark and mostly forms inclusions in chalcopyrite I (Pl. 9, Figs 2 and 2a). It was also found as small grains near chalcopyrite (Pl. 10, Fig. 1), and then it contains small inclusions of chalcopyrite.

Native bismuth, variety I, primarily originated in liquid state, as indicated by characteristic twins (Godovikov & Kolonin 1965); it occurs between quartz grains (Pl. 12, Fig. 2), in bismuthite grains (Pl. 10, Fig. 2) and inside bismuth sulfosalts (Pl. 11, Fig. 3). Variety II was found in fine-grained aggregates in altered parts of bismuthite or Bi-sulfosalts (Pl. 11, Fig. 2).

Bismuthite was formed later than magnetite II (Pl. 10, Fig. 3) and wolframite, syngenetically with molybdenite (Pl. 10, Figs 2 and 4), Bi-sulfosalts and native bismuth I, being in part earlier than scheelite.

Bismuth sulfosalts are probably two different minerals. One of them was identified, chemically and by the X-ray powder analysis, as probable emplectite. They are later than wolframite (Pl. 12, Fig. 1) and magnetite II (Pl. 11, Fig. 2). Sulfosalts are in paragenesis with molybdenite (Pl. 11, Fig. 1) and probably with native bismuth I (Pl. 11, Fig. 3).

Melnikovite and post-pyrrhotitic pyrite are the products of pyrrhotite hydrothermal alteration (Pl. 11, Fig. 4). The relics of pyrrhotite are preserved in the post-pyrrhotitic pyrite (Pl. 7, Fig. 4; Pl. 8, Figs 3 and 4).

Marcasite was found rarely in post-pyrrhotitic pyrite of collomorph structure.

Chalcocite results from the alteration of chalcopyrite II.

As secondary minerals, mostly of hypergenic origin, were ascertained: bismuth ochre (a mixture of some secondary, bismuth minerals; Pl. 12, Figs 3 and 4), and molybdic ochre that covers molybdenite in weathered aplogranites, and finally limonite.
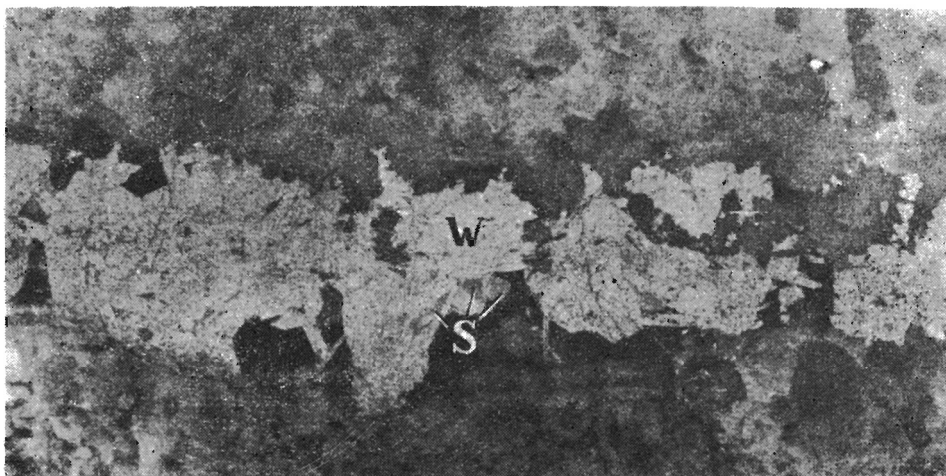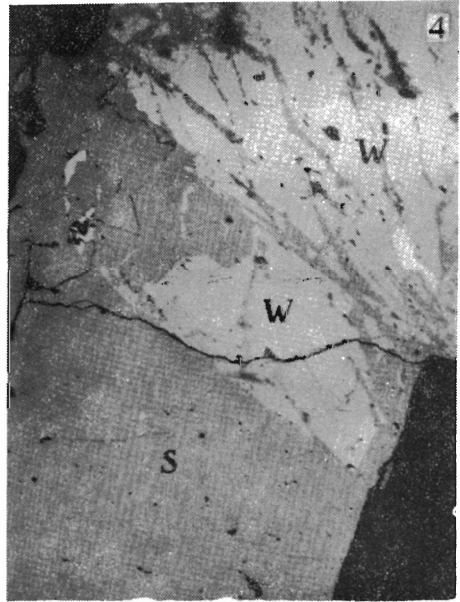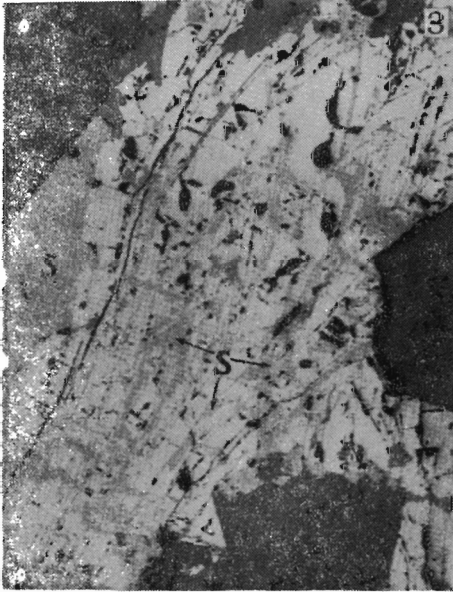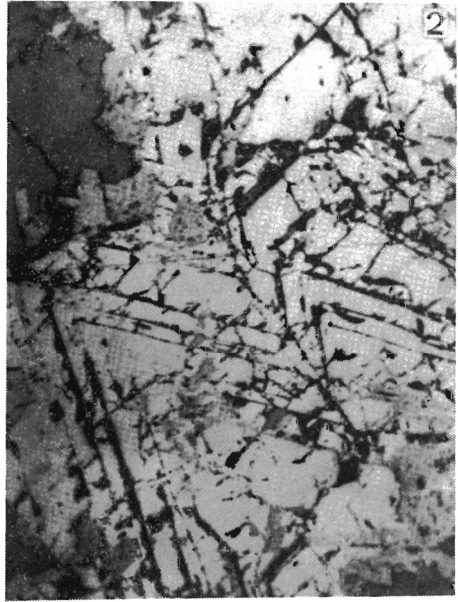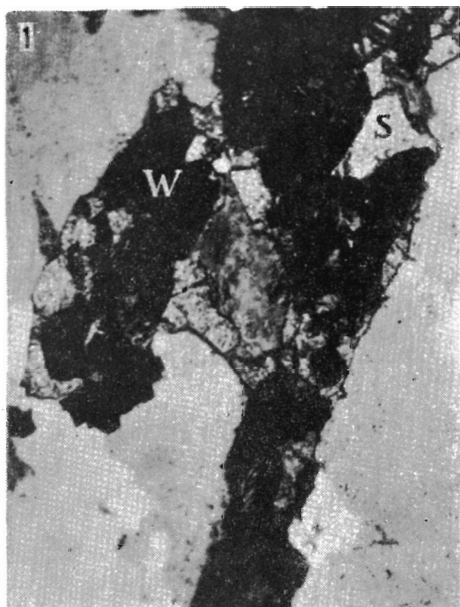

Fig. 7. Wolframite (w) and scheelite (s) in quartz vein from aplogranite; × 4

1-2 — Zonated wolframite in low degree replaced by scheelite; reflected light, × 120.
3 — Zonated wolframite strongly altered into scheelite (s); reflected light, × 120.
4 — Relics of wolframite (w) in scheelite (s), from aplogranite; reflected light, × 120.
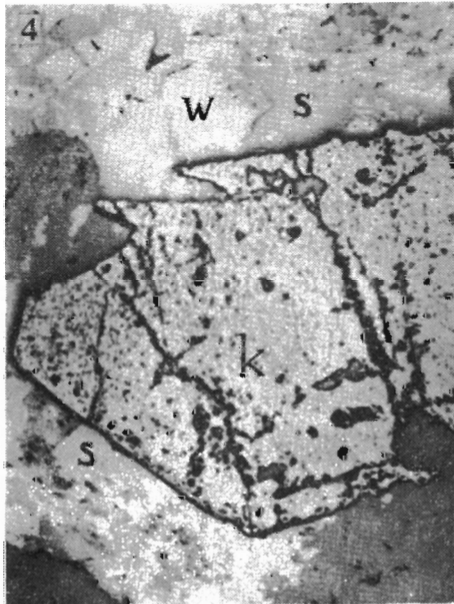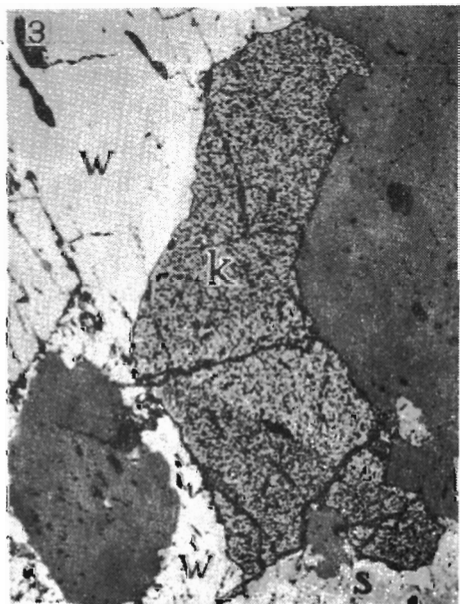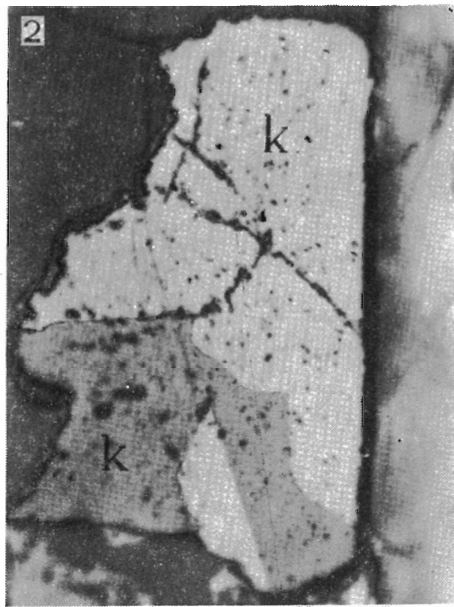
1 — Wolframite (*w*) alteration into scheelite (*s*); transmitted light, nicols oblique, × 120.
2 — Twinned cassiterite (*k*) in quartz; reflected light, × 250.
3-4 — Cassiterite (*k*) and wolframite (*w*) replaced by scheelite (*s*); gray — quartz; reflected light, × 120.
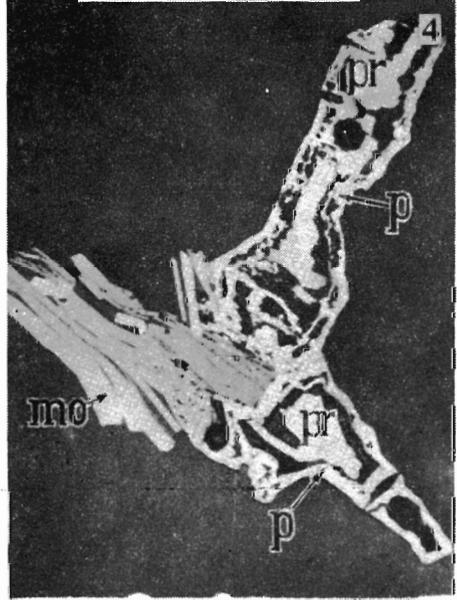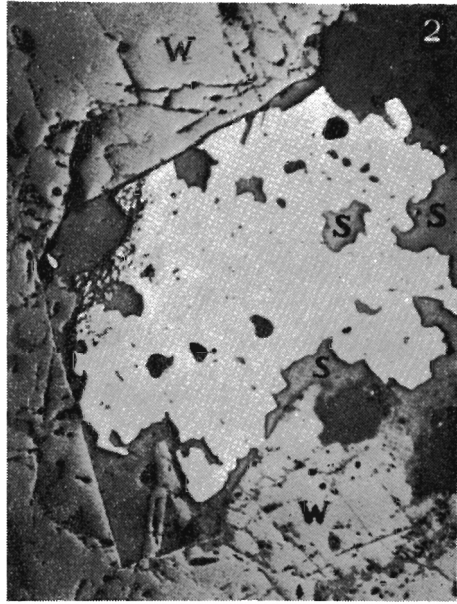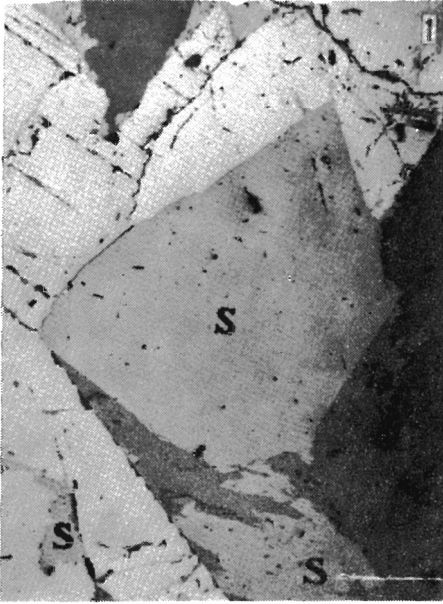
1 — Scheelite (s) between wolframite grains (white); reflected light, × 120.
2 — Pyrite (white) with scheelite (s) and wolframite (w); reflected light, × 120.
3 — Molybdenite (white) with Bi-sulfosalts (sb) in scheelite (s) with preserved relics
   of wolframite (w); reflected light, × 120.
4 — Molybdenite (mo) with pyrrholite (pr) passing into pyrite (p); reflected light,
   × 120.
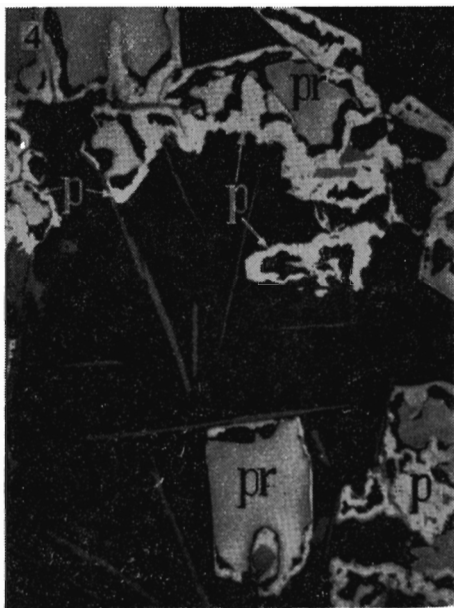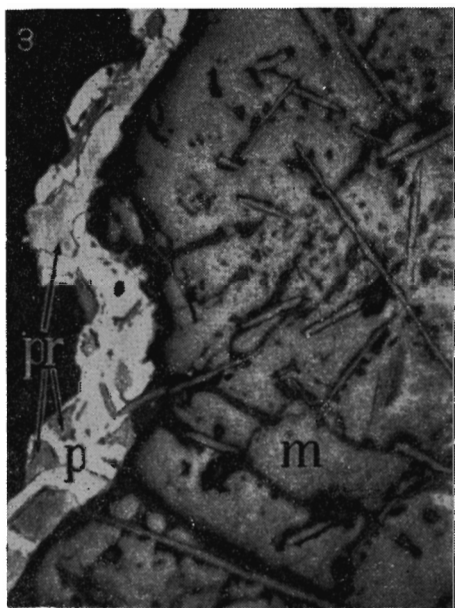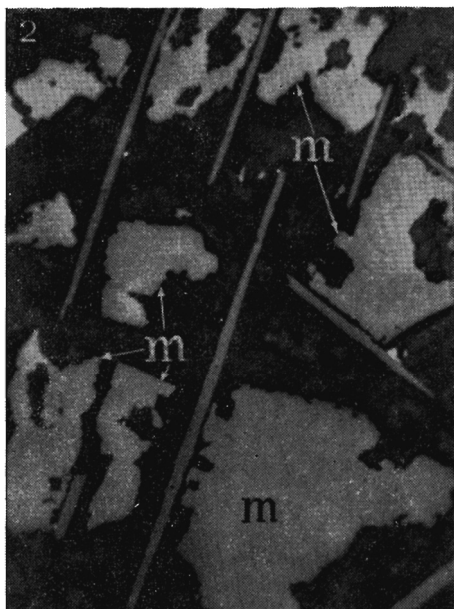
1 — Magnetite I (m) and ilmenite (i); reflected light, × 250.
2 — Grains of magnetite I (m) between ilmenite lamellae; reflected light, × 120.
3 — Pyrrhotite (pr) overgrowing magnetite I (m) with ilmenite lamellae and partly replaced by pyrite (p); reflected light, × 120.
4 — Lamellae of ilmenite in chlorite and pyrrhotite (pr) replaced by pyrite (p); reflected light, × 120.
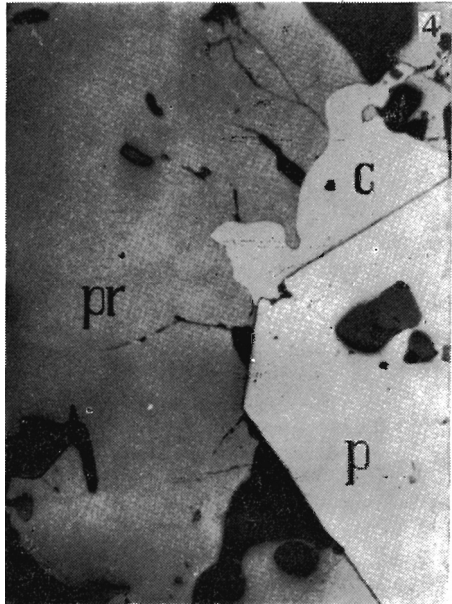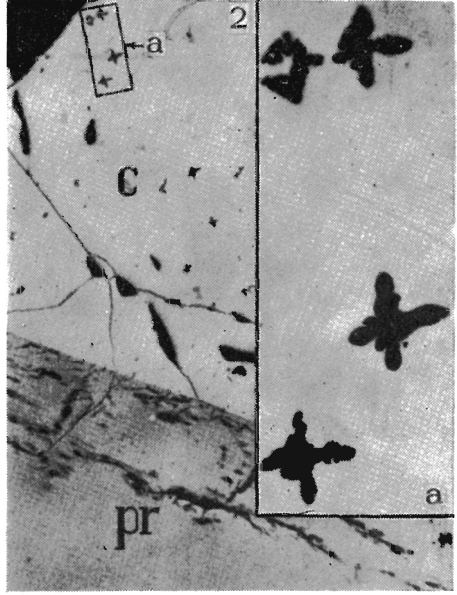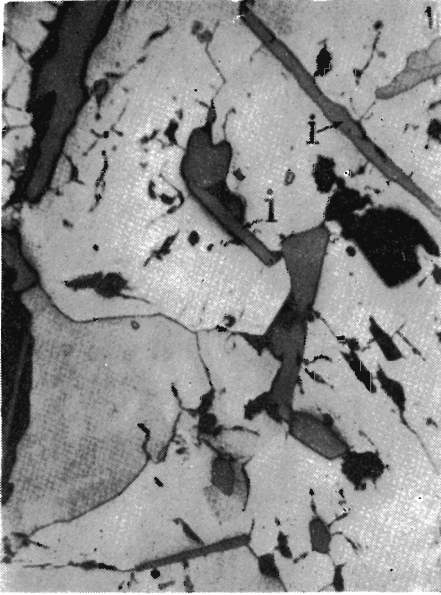
1 — Ilmenite (i) between pyrrhotite grains; reflected light, × 120.
2 — Occurrence of pyrrhotite (pr) and chalcopyrite I (c), containing exsoluted sphalerite "asterisks", × 120 (rectangled area **a**; magnified × 1000 in Fig. 2a); reflected light.
3 — Lamellar structure of pyrrhotite well visible on oxidized surface (upper right grain without lamellar structure); reflected light, × 120.
4 — Occurrence of pyrrhotite (pr), pyrite (p) and chalcopyrite I (c), reflected light, × 60.
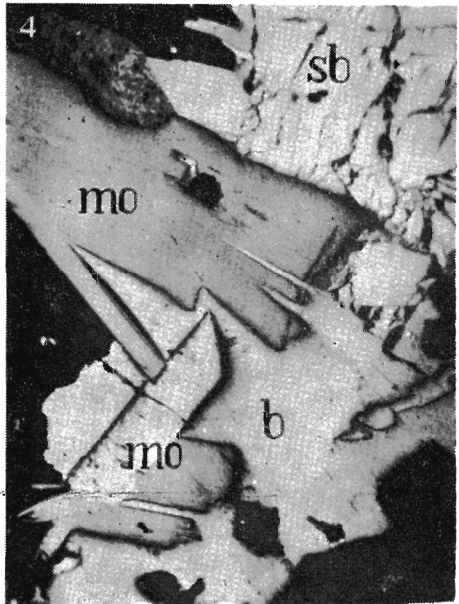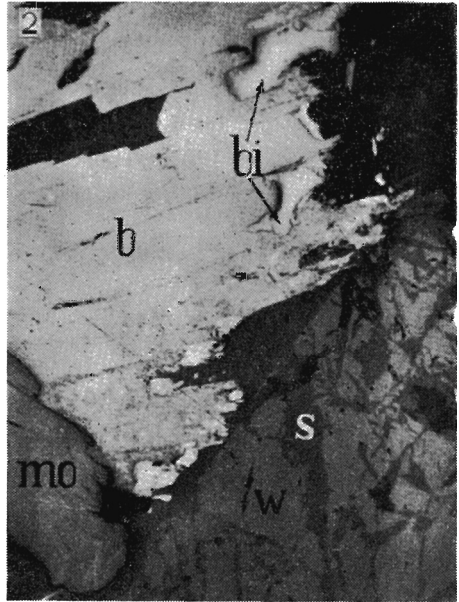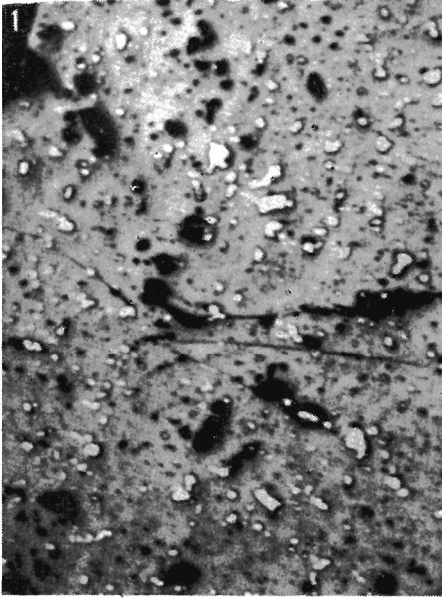
1 — Chalcopyrite *I* (white) in sphalerite (gray); black — non-ore minerals; reflected light, × 250.
2 — Native bismuth *I* (*bi*) in bismuthite (*b*) occurring together with molybdenite (*mo*) and wolframite (*w*) altering into scheelite (*s*); reflected light, × 120.
3 — Bismuthite (white) between grains of magnetite *II* (*m*) and mushketovite (*mu*); reflected light, × 120.
4 — Molybdenite (*mo*) with bismuthite (*b*) and Bi-sulfosalts (*sb*); reflected light, × 250.
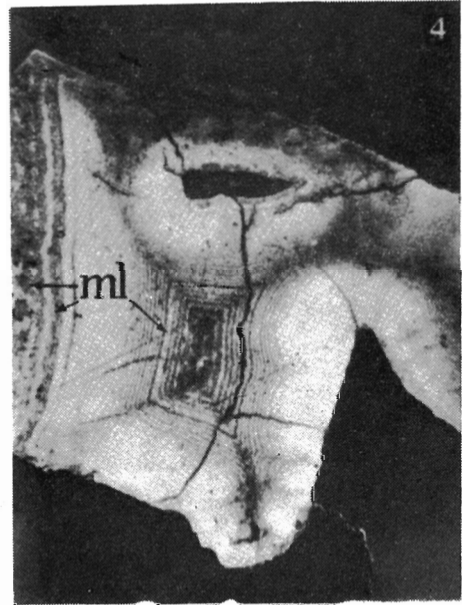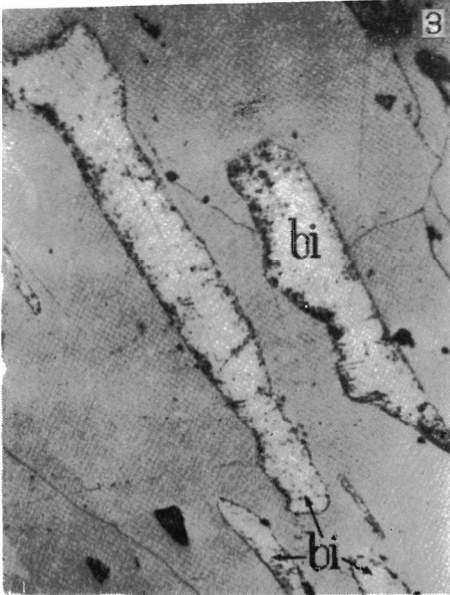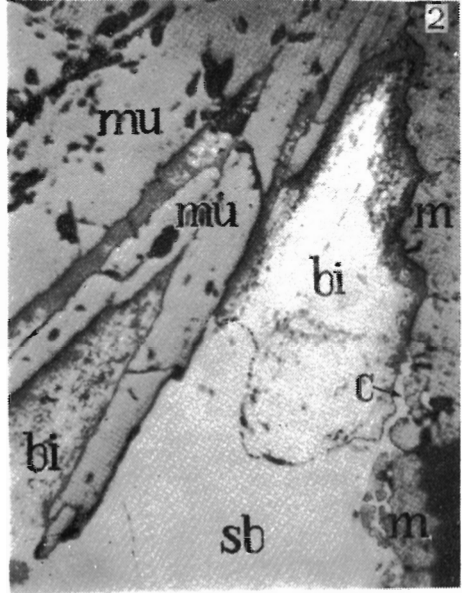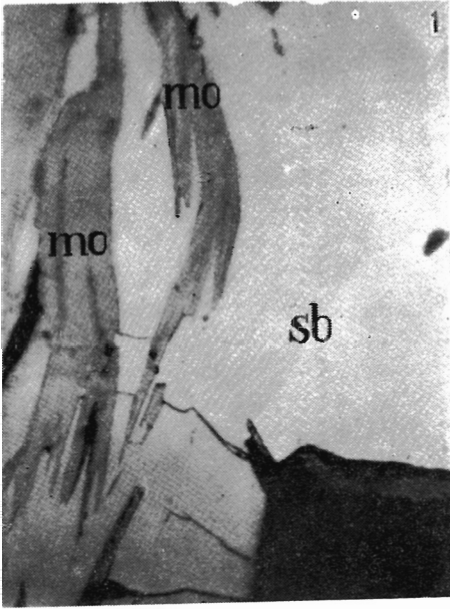
1 — Molybdenite (*mo*) in Bi-sulfosalt (*sb*); reflected light, × 250.
2 — Bi-sulfosalt (*sb*), native bismuth *II* (*bi*) and chalcopyrite *I* (*c*) between mush-ketovite (*mu*) and magnetite *II* (*m*); reflected light, × 120.
3 — Native bismuth *I* (*bi*) in Bi-sulfosalt; reflected light, × 250.
4 — Pseudomorph of post-pyrrhotitic pyrite with preserved melnikovite (*ml*); reflected light, × 120.
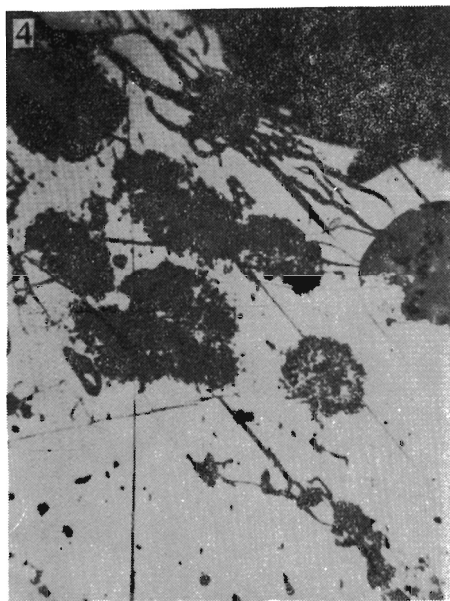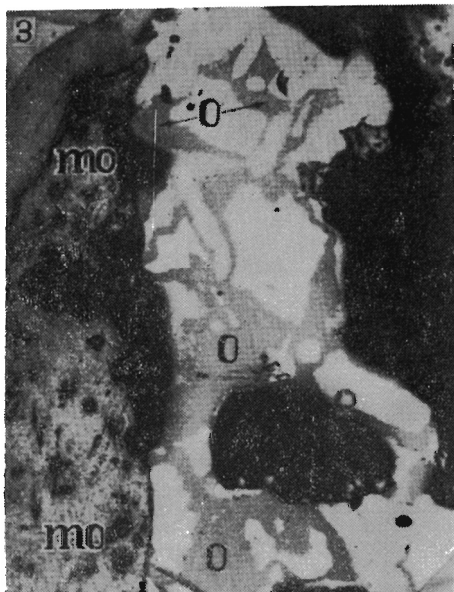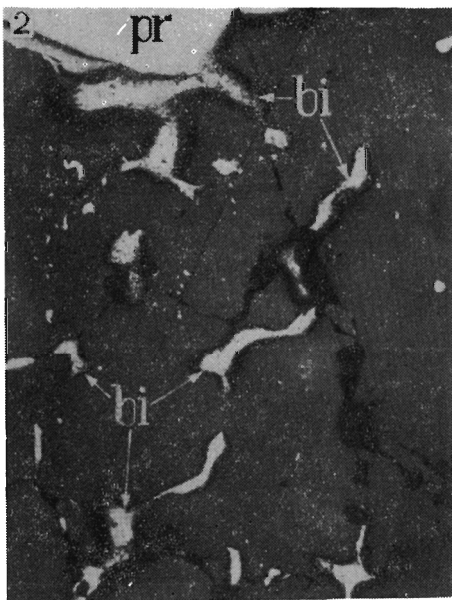
1 — Bi-sulfosalts (white) among wolframite (*w*); reflected light; × 120.
2 — Native bismuth *I* (*bi*) near pyrrhotite (*pr*) in quartz (gray); reflected light, × 250.
3 — Bi-sulfosalt (white) replaced by bismuth ochre (*o*); *mo* — molybdenite; reflected light, × 120.
4 — Bismuthite (white) replaced by secondary minerals; reflected light, × 60.

CONDITIONS OF ORE MINERALIZATION

The investigated ore–bearing aplogranites crystallized from the remnant silicate melt, bearing a correspondingly large amount of volatile components which then formed post-magmatic, mostly aqueous parent solutions of ore parageneses. The primary solutions were of pneumatolytic nature at a temperature dropping from 480°C. At that stage such minerals crystallized as quartz (partly), the majority of feldspars in vugs, magnetite *I* and ilmenite (Fig. 8). The pH-values oscillated near the
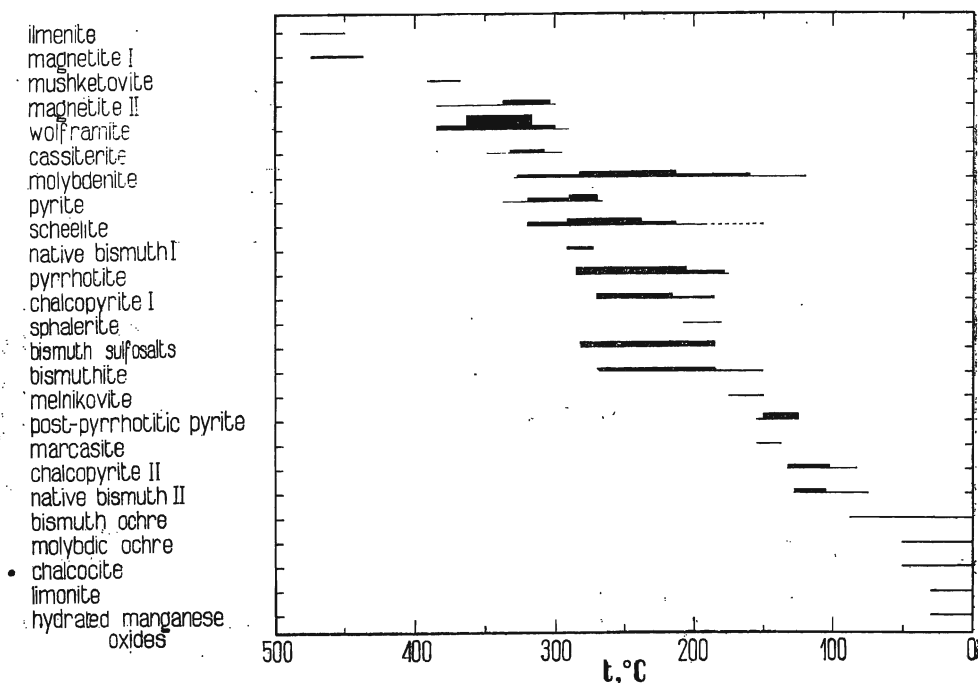
Fig. 8. Crystallization sequence of the investigated ore minerals

neutral and Eh was slightly higher than zero. A slight increase in redox potential caused then the crystallization of hematite.

As follows from a comparison with P-T conditions of the origin of some typical deposits (Figs 9 and 10), after condensation at a temperature about 380°C the solutions became liquid, i.e. hydrothermal, and the conditions arose favorable to the origin of tungsten and tin minerals. The beginning of wolframite and the origin of cassiterite crytallizing later partly together with magnetite *II* are associated with the condensation. The lowered Eh values also cause the alteration of hematite into mushketovite.

wolframite

Locality	References	t. °C 100 200 300 400 500
Szklarska Por.	—	
Krušne Mts	10,15	
Zabaikale	8,10	
S Caucasus	10	
S Ural		
Kaz.SSR	7,10	
Chukotka	10	
Altai	12	
Mongolia	2,10	
China	10	
Japan	4,5	
Generalized	14	

cassiterite

Szklarska Por.	—	
Krušne Mts	1,3,10,15	
Zabaikale	10,11	
Chukotka	9,10,11	
S Sichote Alin	11	
S Ussuri		
Ezop		
Mongolia	10	
Japan	4,5,13	
Bolivia	6	
Generalized	14	

100   200   300   400   500
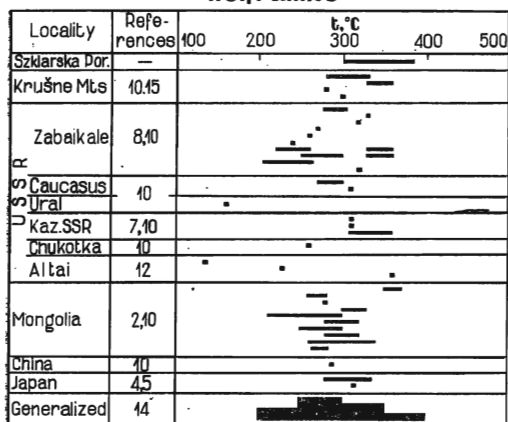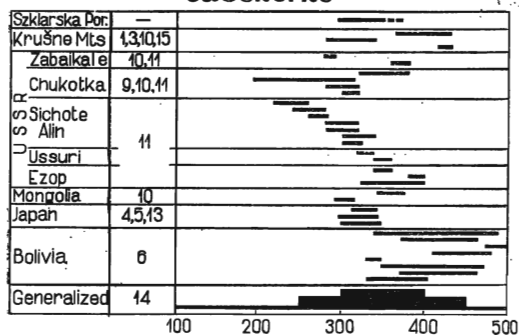
Fig. 9. Crystallization temperatures of wolframite and cassiterite in some ore deposits as appear from references: 1 — Bogoyavlenskaya & al. (1973), 2 — Dashdavaa (1970), 3 — Durišová (1971), 4 — Imai (1970), 5 — Imai & Takenouchi (1971), 6 — Kelly & Turneaure (1970), 7 — Kostyleva (1965), 8 — Lazko & al. (1972), 9 — Nauchitel & al. (1972), 10 — Naumov & Ivanova (1971), 11 — Ryabov (1968), 12 — Sotnikov & Nikitina (1971), 13 — Takenouchi (1971), 14 — Tugarinov & Naumov (1973), 15 — Ulrichová & Bradač (1971)

The composition of early solution was probably of sodium — chloride nature with significant amounts of Fe. This solution was replaced by a hydrothermal fluid bearing tungstate ions, precipitating together with Fe and Mn as wolframite. In general, tungsten can be transported under moderately acid to weakly alkaline conditions (cf. Bryzgalin 1967,

Fig. 10. The P-t conditions of wolframite crystallization in some wolframite deposits
1 — Szklarska Poręba Huta, 2 — Spokoynoe, 3 — Belukha, 4 — Bukuka, 5 — Yultin, 6 — Khara-Moritu, 7 — Buren-Tsogto, 8 — Chulun-Khuryete, 9 — Modoto, 10 — Ikh-Khayerkhan (2—9 after Naumov & Ivanova 1971, 10 — after Dashdavaa 1970, Naumov & Ivanova 1971)
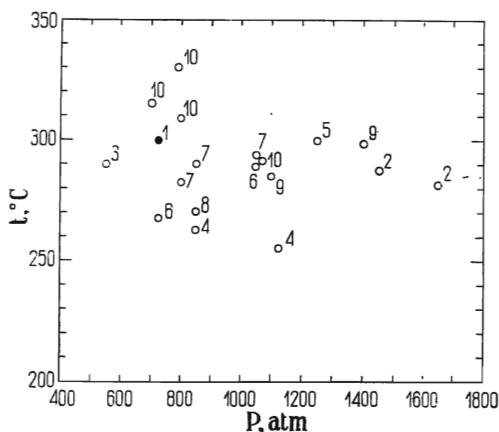
Ivanova 1972). In the paragenesis under study there are no distinct signs, indicating the range of pH values during wolframite crystallization. The occurrence of wolframite and molybdenite may be helpful to a certain extent, since the ions of either WO_4^{2-} or $WO_2S_2^{2-}$ can coexist with MoS_4^{2-}-ions under alkaline conditions (Pavlov & Sharapov 1973). Molybdenite started precipitating when the solution became rather acid and reducing. The thesis on a low Eh value at about 300°C is supported by the occurrence of native bismuth, precipitating as a liquid phase in the paragenesis.

Scheelite crystallized partly together with molybdenite because of an increasing activity of Ca^{2+}-ions in the solution resulting from the replacement of Ca by Na in plagioclases. The Ca^{2+}-ions attacked wolframite forming scheelite and releasing Fe-ions into solution. Iron, did not hold now in wolframite, formed magnetite *II*, pyrite, and later — pyrrhotite and chalcopyrite *I*. A pressure at that stage (*c*. 300°C) amounted to about 725 atm.

In the cooling hydrothermal solution, the slightly increasing Eh potential caused crystallization of bismuthite and Bi-sulfosalts. The essential crystallization of sulfides finished at about 200°C and 680 atm because of a lack of metals, whereas a relatively high activity of S^{2-}-ions caused the alteration of pyrrhotite into melnikovite. The subsequent decrease in S^{2-} activity partly with lower values of Eh and a recurrence of certain metals yielded such minerals as native bismuth *II* and chalcopyrite *II*. This hydrothermal ore mineral assemblage has subsequently been submitted to the hypergenic alteration.

The ore mineralization investigated and the parent rocks are typical of W–Sn–Mo deposits being the differentiated intrusive with an aplite-like zone and quartz ore-bearing veins (*cf*. Leontev 1972).

Institute of Geochemistry, Mineralogy and Petrography   *Institute of Geology*
of the Warsaw University   *of the Warsaw University*
(A. Kozłowski & Ł. Karwowski)   *(W. Olszyński)*
Al. Żwirki i Wigury 93, 02-089 Warszawa, Poland
Warsaw, February 1975

REFERENCES

ARNOLD R. G. 1969. Pyrrhotite phase relations below 304±6°C 1 atm total pressure. *Econ. Geol.*, 64 (4), 405—419. Lancaster.

BARABANOV V. F. 1960. To the question of determining the composition of the wolframite by its specific gravity. *Vestn. Leningr. Univ., Geol. Geogr.*, 12 (2), 149—151. Leningrad.

— 1961. Mineralogia volframitovykh mestorozhdenii Vostochnogo Zabaikalya (Bukuka-Belukha). [in Russian]. Izd. Leningr. Univ., 112—126. Leningrad.

— & SYRITSO L. F. 1966. The influence of niobium, tantalum and scandium on the specific gravity of wolframite. Zap. Vses. Mineral. Obshch., 95 (5), 578—583. Moskva — Leningrad.

BOGOYAVLENSKAYA I. V., DOLOMANOVA E. I. & LOSEVA T. I. 1973. K voprosu o fiziko-khimicheskikh usloviakh formirovania olovyanogo mestorozhdenia Ehrenfriedersdorf (GDR) po gazovo-zhidkim vklucheniam v mineralakh. Tezisy dokladov IV Regionalnogo soveshchania po termobarogeokhimii processov mineraloobrazovania [in Russian]. Izd. Rostovsk. Univ. Rostov.

BRYZGALIN O. V. 1967. O vliyanii sostava rastvorov na formu perenosa volframa v gidrotermalnykh usloviakh [in Russian]. Mineralogia i geokhimia volframitovykh mestorozhdenii, 69—72. Izd. Leningr. Univ. Leningrad.

DANA J. D. & DANA E. S. 1946. The system of mineralogy. New York.

DASHDAVAA S. 1970. Types of mineral formation solution inclusions in wolframite and some features of quartz-wolframite veins in the Ih-Haierhan deposit, Mongolia. Mineral. Sb. Lvovsk. Univ., 24 (2), 236—238. Lvov.

DURIŠOVÁ J. 1971. Geothermometric study of cassiterite from the Preiselberk deposit in the eastern part of the Krušne Hory Mts. Věst. Ústřed. Úst. Geol., 46 (6), 223—228. Praha.

GODOVIKOV A. A. & KOLONIN G. P. 1965. Experimental investigations of peculiarities of bismuth extraction and possibilities of its application as geological thermometer. Geol. Rud. Mestorozhd., No. 2, 97—101. Moskva.

IMAI H. 1970. Geology and mineral deposits of the Akenobe mine. IMA 7th General Meeting, IAGOD Tokyo-Kyoto Meeting, Guidebook 8, Excursion B4, 1—21. Tokyo.

— & TAKENOUCHI S. 1971. Report of the Japanese Committee on the Inclusions in Minerals. J. Mining Metall. Inst. Japan, 87 (1001), 546—560. Tokyo.

IVANOVA G. F. 1972. Geokhimicheskie uslovia obrazovania volframitovykh mestorozhdenii [in Russian]. Nauka, 101—116. Moskva.

KALYUZHNYI V. A. 1960. Metody vivchennia bogatofazovikh vkluchen u mineralakh [in Ukrainian]. Vid. AN USSR, 28—86. Kiïv.

KARWOWSKI Ł., OLSZYŃSKI W. & KOZŁOWSKI A. 1973. Wolframite mineralizatlion from the vicinity of Szklarska Poręba Huta. Przegl. Geol., No. 12, 633—637. Warszawa.

KELLY W. C. & TURNEAURE F. S. 1970. Mineralogy, paragenesis and geothermometry of the tin and tungsten deposits of the eastern Andes, Bolivia. Econ. Geol., 65 (6), 609—680. Lancaster.

KOSTYLEVA E. E. 1965. Metod dekrepitatsii i ego znachenie dla mineralogicheskoj termometrii [in Russian]. Mineral. termometria i barometria, Vol. 1. Nauka. Moskva.

LAZKO E. M., DOROSHENKO U. P., KOLTUN L. I., LYAKHOV U. V., MYAZ N. I. & PIZNIUR A. V. 1972. O temperaturnykh i drugikh fiziko-khimicheskikh usloviakh formirovania postmagmaticheskikh mestorozhdenii Vostochnogo Zabaikalya [in Russian]. Rudoobrazuyushchaya sreda po vklucheniam v mineralakh, 15—23. Nauka. Moskva.

LEONTEV A. N. 1972. Tipovaya geokhimicheskaya model rudonosnogo granitnogo intruziva i ee petrograficheskie modifikatsii [in Russian]. Magmatizm, formatsii kristallicheskikh porod i glubiny Zemli, Vol. 2, 9—12. Nauka. Moskva.

MAKSIMIUK E. I. 1971. Zavisimost fizicheskikh svoistv volframita ot khimicheskogo sostava [in Russian]. Mineralogia i geokhimia volframovykh mestorozhdenii, 275—281. Izd. Leningr. Univ. Leningrad.

MOENKE H. 1960. Ultrarotspekralphotometer als Hilfsmittel bei der Prospektion und Erzlagestätten. Jahrb. 11, 402—406. Jena.

NAUCHITEL M. A., LUGOV S. F., MAKEEV B. V. & POTAPOVA T. M. 1972. Temperaturnye uslovia formirovania olovorudnykh mestorozhdenii kassiterit--kvartsevoi formatsii Severo-Vostoka SSSR [in Russian]. Rudoobrazuyushchaya sreda po vklucheniam v mineralakh, 97—106. Nauka. Moskva.

NAUMOV V. B. 1968. K voprosu ob opredelenii temperatur mineraloobrazovania metodom dekrepitatsii [in Russian]. Mineral. termometria i barometria, Vol. 2, 37—43. Nauka. Moskva.

— & MALININ S. D. 1968. A new method of pressure determination by gaseous--liquid insclusions. Geokhimia, No. 4, 432—441. Moskva.

— & IVANOVA G. F. 1971. Barothermometric characteristics of the conditions of wolframite deposit formation. Geokhimia, No. 6, 627—641. Moskva.

PAVLOV A. L. & SHARAPOV V. N. 1972. Elementy fiziki i fizikokhimii protsessov formirovania redkometalnykh mestorozhdenii zhilno-greizenovogo tipa [in Russian]. Trudy IGiG, 114, 73—136. Moskva.

PENDIAS H. & WALENCZAK Z. 1956. Signs of mineralization in the north-western part of Strzegom massif, Lower Silesia. Biul. Inst. Geol., No. 112, 209—240. Warszawa.

POLAŃSKI A. & SMULIKOWSKI K. 1969. Geochemia. Wyd. Geol. Warszawa.

RYABOV V. K. 1968. Temperaturnoe raionirovanie v olovonosnykh provintsyakh s pomoshchyu termozvukovogo metoda [in Russian]. Mineral. termometria i barometria, Vol. 1, 271—275. Nauka. Moskva.

SOTNIKOV V. I. & NIKITINA E. I. 1971. Molybdenum — rare metal — tungsten (greisen) formation of Mountainous Altai. Nauka. Moskva.

SYRITSO L. F. 1967. Volframovaya mineralizatsia odnogo iz redkometalnykh mestorozhdenii Zabaikalya [in Russian]. Mineralogia i geokhimia volframovykh mestorozhdenii, 41—55. Izd. Leningr. Univ. Leningrad.

TAKENOUCHI S. 1971. Study of CO_2-bearing fluid inclusions by means of the freezing stage microscope. Kodzan Tisitsu (Mining Geol.,), 21, 28—42. Tokyo.

TETYAEV M. M. 1918. Volframovye i olovyanye mestorozhdenia Onon.-Borzinskogo raiona Zabaikalskoi oblasti [in Russian]. Mat. po obshch. i prikl. geol., Vol. 32. Petrograd.

TUGARINOV A. I. & NAUMOV V. B. 1973. Fiziko-khimicheskie parametry gidrotermalnogo mineraloobrazovania [in Russian]. Mezhdunarodnyj Geokhimicheskij Kongress, Moskva 1971, Doklady, Vol. 2, 7—19. Izd. AN SSSR. Moskva.

ULRÍCHOVÁ D. & BRADÁČ L. 1971. Decrepitation and optical methods applied to inclusions in minerals. Věstn. Ústřed. Úst. Geol., 46 (4), 193—208. Praha.

A. KOZŁOWSKI, Ł. KARWOWSKI i W. OLSZYŃSKI

OKRUSZCOWANIE APLOGRANITÓW OKOLIC SZKLARSKIEJ PORĘBY

(Streszczenie)

W pracy przedstawiono wyniki badań nad strefą okruszcowanych aplogranitów okolic Szklarskiej Poręby w Karkonoszach (fig. 1). W aplogranitach tych, wykazujących przejawy metasomatozy sodowej (por. pl. 1 i 4), oraz w żyłach kwarcowych (fig. 2 i 7) stwierdzono obecność m.in. takich minerałów kruszcowych, jak: wolframit, kasyteryt, molibdenit, szelit, bizmut rodzimy, bizmutyn, pirotyn, chalkopiryt oraz siarkosole bizmutowe (por. fig. 5—6 i pl. 5—12). Na podstawie badań inkluzji fluidalnych (por. pl. 2—3) wykazano, że minerały kruszcowe krystalizowały tutaj z rozcieńczonych roztworów chlorkowo-fluorkowo-siarczkowych (głównie kationy: Na, Ca, K, Al) przy ciśnieniach rzędu 700 atm w temperaturach 400—100°C (por. fig. 3 i 8). Stwierdzono typowość hydrotermalnych warunków powstania badanych kruszców w stosunku do innych znanych tego typu złóż wolframitowo-kasyterytowo-molibdenitowych na świecie (por. fig. 4, 9 i 10).